Journal of Magnetism and Magnetic Materials 322 (2010) 603–608

Contents lists available at ScienceDirect

Journal of Magnetism and Magnetic Materials

journal homepage: www.elsevier.com/locate/jmmm

Regular Submission

Influence of external magnetic field on magnon–plasmon polaritons in negative-index antiferromagnet–semiconductor superlattices

R.H. Tarkhanyan [a,*], D.G. Niarchos [b], M. Kafesaki [a]

[a] Institute of Electronic Structure and Laser-FORTH, Heraklion, Crete 71110, Greece
[b] Institute of Materials Science, NCSR "Demokritos", Athens 15310, Greece

ARTICLE INFO

Article history:
Received 31 July 2009
Received in revised form
30 September 2009
Available online 22 October 2009

Keywords:
Negative refraction
Magnon–plasmon polaritons
Superlattice
Semiconductor
Antiferromagnet

ABSTRACT

The peculiarities of the negative refraction in periodic multilayered antiferromagnet–semiconductor nanostructures are investigated in the presence of an external magnetic field parallel to the plane of the layers. Effective material tensors are obtained using method of anisotropic homogeneous medium. Dispersion and energetic relations for the mixed magnon–plasmon polaritons are investigated in the case of the Voigt geometry. Frequency regions of anomalous dispersion are found and studied in various regimes of the applied magnetic field. The necessary conditions are found under which the structure behaves as a left-handed negative-index metamaterial. Analytical expressions for the frequency-dependent phase and group refractive indices are obtained.

1. Introduction

During the last years, the exotic behavior of electromagnetic waves (EMW) in so called left-handed media became an object of many interesting and outstanding investigations (see, for example, [1–11] and citations therein). In particular, a great effort has been made to predict theoretically and observe the negative refraction (NR) of the waves in various artificial materials including periodic multilayer nanostructures, where the waves have many unusual properties due to their specific dispersion characteristics. In Ref. [12], the problem of anomalous refraction has been studied in ferrite-semiconductor superlattices (SL) in the presence of an external magnetic field and has been shown that the latter influences considerably on the dispersion properties of the waves as well as on the number of the spectral branches and frequency regions of existence for the backward waves. On the other side, in the last several years there has been enormous interest in antiferromagnetic substances, which possess special optical and spintronic properties in terahertz frequency region. In spite of that, up to now there are only a few studies on the possibility of NR in periodic structures containing antiferromagnetic layers. In [13], the characteristics of the bulk EMW have been discussed in antiferromagnet/semiconductor SL in the absence of an external magnetic field. The properties of the magnetic plasmon polaritons in homogeneous negative-index metallic antiferromagnets have been studied in [14].

The aim of this work is an investigation of the effect of an external static magnetic field on the behavior of EMW in periodic multilayer nanostructures consisting of alternating layers of antiferromagnetic insulator (for example, $Cd_{1-x}Mn_xTe$) and nonmagnetic semiconductor (CdTe). When the characteristic dimensions of the layers are much smaller than the internal wavelength, the coexistence of both magnetic and plasmonic properties in such structures leads to the interesting peculiarities of the waves propagating in the backward regime. We shall examine the anomalous refraction of the coupled magnon–plasmon polaritons, that is, photons coupled with antiferromagnetic magnons and magnetoplasmons. As it is well known [15,16], this coupling is especially strong for the waves in Thz region, when frequencies of the photons are comparable with the characteristic frequencies of the magnons and magnetoplasmons.

The paper is organized in five main sections. Section 2 describes the effective permittivity and permeability tensors of SL used for the analysis of the dispersion relations for the propagating waves. Section 3 discusses mixed magnon–plasmon polaritons in the case of the Voigt geometry when TE- and TM-type polarized waves propagate separately. The dispersion curves and frequency regions of existence are determined for TE waves, which can exhibit anomalous dispersion. In Section 4, the necessary conditions are obtained for absolute left-handed behavior of the medium with respect to the TE waves. In Section 5 the concluded remarks are highlighted.

* Corresponding author. Present address: 5 Arkadiou (Pellinis), Piraeus 18534, Greece. Tel.: +30 2104179379.
E-mail address: rolandtarkhanyan@yahoo.com (R.H. Tarkhanyan).

0304-8853/$ - see front matter © 2009 Elsevier B.V. All rights reserved.
doi:10.1016/j.jmmm.2009.10.023

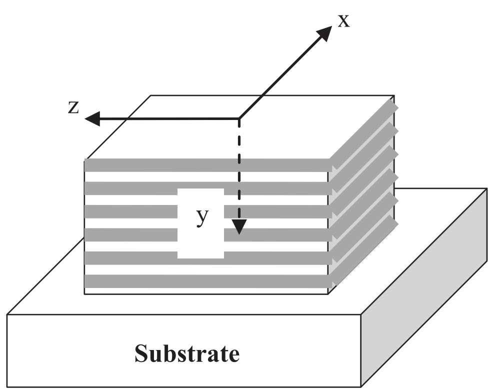

Fig. 1. Geometry of the problem. The static magnetic field is parallel to the z-axis.

2. Effective material tensors

The biasing magnetostatic field $\mathbf{B}_0||\mathbf{z}$ is assumed to be parallel to the plane of the layers and along the positive z-axis (see Fig. 1). We will make simplifying assumptions that B_0 is less than the spin-flop field and the medium is lossless. Also we assume that: (1) semiconductor layers contain only one type of free charge carriers with a parabolic conduction band; (2) antiferromagnetic layers with two antiparallel magnetic sublattices have an 'easy-axis' type magnetic anisotropy, so as the saturation magnetization $\mathbf{M}_S$, anisotropy field $\mathbf{H}_A$ and exchange field $\mathbf{H}_E$ are oriented in the same direction along the static field $\mathbf{H}_0$. Then, an individual nonmagnetic semiconductor layer of thickness l_1 can be described by the following permittivity tensor:

$$\hat{\varepsilon} = \begin{pmatrix} \varepsilon_1 & i\varepsilon_2 & 0 \\ -i\varepsilon_2 & \varepsilon_1 & 0 \\ 0 & 0 & \varepsilon_3 \end{pmatrix}, \tag{1}$$

where

$$\varepsilon_1 = \varepsilon_\infty\left(1 - \frac{\omega_p^2}{\omega^2 - \omega_c^2}\right), \quad \varepsilon_2 = -\frac{\varepsilon_\infty \omega_c \omega_p^2}{\omega(\omega^2 - \omega_c^2)}, \quad \varepsilon_3 = \varepsilon_\infty\left(1 - \frac{\omega_p^2}{\omega^2}\right). \tag{2}$$

$\omega_p = (Ne^2/m\varepsilon_0\varepsilon_\infty)^{1/2}$ is the plasma frequency, $\omega_c = eB_0/m$ is the cyclotron frequency, e, m and N are the charge, effective mass and density of the conduction electrons, respectively, $B_0 = \mu_0 H_0$, ε_∞ is the high-frequency dielectric constant, ε_0 and μ_0, respectively, are permittivity and permeability of the free space.

An individual antiferromagnetic layer of thickness l_2 is described by a scalar dielectric constant ε_A and permeability tensor [17,18].

$$\hat{\mu} = \begin{pmatrix} \mu_1 & i\mu_2 & 0 \\ -i\mu_2 & \mu_1 & 0 \\ 0 & 0 & 1 \end{pmatrix}, \tag{3}$$

where

$$\mu_1 = 1 + \omega_A\omega_S\left[\frac{1}{\omega_T^2 - (\omega+\omega_0)^2} + \frac{1}{\omega_T^2 - (\omega-\omega_0)^2}\right], \tag{4a}$$

$$\mu_2 = \omega_A\omega_S\left[\frac{1}{\omega_T^2 - (\omega+\omega_0)^2} - \frac{1}{\omega_T^2 - (\omega-\omega_0)^2}\right], \tag{4b}$$

$\omega_0 = \gamma H_0$, $\omega_A = \gamma H_A$, $\omega_S = \gamma M_S$, γ is the gyromagnetic ratio, ω is the angular frequency of the waves and

$$\omega_T = \gamma\sqrt{H_A(H_A + 2H_E)}, \tag{4c}$$

is the antiferromagnetic resonance frequency in the absence of an external magnetic field. For most of known antiferromagnetic materials, this characteristical transverse magnon frequency is in the far infrared region. Inserting, for example, the following values:

$$H_E = 550\,\text{kG}, \quad H_A = 3.8\,\text{kG}, \quad \gamma = 2.87\,\text{GHz/kG} \quad (\text{MnF}_2) \tag{4d}$$

from Eq.(4c) we obtain $\omega_T = 185.874$ GHz.

Assuming that the period of the structure $d = l_1 + l_2$ is much smaller than the internal wavelength and using method of effective anisotropic homogeneous medium [19,20,12], we obtain constitutive relations in the form

$$\mathbf{D} = \varepsilon_0\hat{\varepsilon}_{ef}\mathbf{E}, \quad \mathbf{B} = \mu_0\hat{\mu}_{ef}\mathbf{H}, \tag{5}$$

where relative effective permittivity and permeability tensors read

$$\hat{\varepsilon}_{ef} = \begin{pmatrix} \varepsilon_{11} & i\varepsilon_a & 0 \\ -i\varepsilon_a & \varepsilon_{22} & 0 \\ 0 & 0 & \varepsilon_{33} \end{pmatrix}, \quad \hat{\mu}_{ef} = \begin{pmatrix} \mu_{11} & i\mu_a & 0 \\ -i\mu_a & \mu_{22} & 0 \\ 0 & 0 & 1 \end{pmatrix}, \tag{6}$$

$$\varepsilon_{11} = \frac{1}{d}\left[l_1\varepsilon_1 + l_2\varepsilon_A\left(1 - \frac{\varepsilon_2\varepsilon_a}{\varepsilon_A^2}\right)\right], \quad \varepsilon_a = \varepsilon_2\left(1 + \frac{l_2\varepsilon_1}{l_1\varepsilon_A}\right)^{-1}, \tag{6a}$$

$$\varepsilon_{22}^{-1} = \frac{1}{d}\left(\frac{l_1}{\varepsilon_1} + \frac{l_2}{\varepsilon_A}\right), \quad \varepsilon_{33} = \frac{1}{d}(l_1\varepsilon_3 + l_2\varepsilon_A), \tag{6b}$$

$$\mu_{11} = [l_2\mu_1 + l_1(1 - \mu_2\mu_a)]/d, \quad \mu_a = l_2\mu_2/(l_2 + l_1\mu_1),$$
$$\mu_{22}^{-1} = (l_1 + l_2\mu_1^{-1})/d. \tag{6c}$$

The behavior of a monochromatic plane electromagnetic wave $\boldsymbol{E},\boldsymbol{H} \sim \exp[i(\boldsymbol{kr} - \omega t)]$ in the medium described by Eq. (6) can be investigated using the Maxwell equations in the form

$$[\boldsymbol{k} \times \boldsymbol{E}] = \omega\mathbf{B}, \quad [\boldsymbol{k} \times \boldsymbol{H}] = -\omega\mathbf{D}. \tag{7}$$

Eliminating the magnetic field $H = (\omega\mu_0\hat{\mu}_{ef})^{-1}\boldsymbol{k} \times \boldsymbol{E}$ from Eq. (7), for an arbitrary direction of the wave propagation $\boldsymbol{s} = \boldsymbol{k}/k$ we obtain a set of equations

$$(n^2\hat{\eta} - \lambda_m\hat{\varepsilon}_{ef})\boldsymbol{E} = 0, \tag{8}$$

where $n = ck/\omega$ is the refractive index,

$$\lambda_m \equiv \mu_{11}\mu_{22} - \mu_a^2, \tag{9a}$$

and

$$\hat{\eta} = \begin{pmatrix} \mu_{11}s_z^2 + \lambda_m s_y^2 & -(\lambda_m s_x s_y + i\mu_a s_z^2) & -s_z(\mu_{11}s_x - i\mu_a s_y) \\ -\lambda_m s_x s_y + i\mu_a s_z^2 & \mu_{22}s_z^2 + \lambda_m s_x^2 & -s_z(\mu_{22}s_y + i\mu_a s_x) \\ -s_z(\mu_{11}s_x + i\mu_a s_y) & -s_z(\mu_{22}s_y - i\mu_a s_x) & \mu_{11}s_x^2 + \mu_{22}s_y^2 \end{pmatrix}. \tag{9b}$$

The system of equations (8) has a nontrivial solution only if the determinant of the coefficient matrix vanishes

$$\text{Det}\,\|n^2\eta_{ij} - \lambda_m(\varepsilon_{ef})_{ij}\| = 0. \tag{10}$$

Using Eqs. (9b) and (6) for the tensor $\hat{\varepsilon}_{ef}$, we can write Eq. (10) in the form

$$An^4 - \lambda_m Bn^2 + \varepsilon_{33}\lambda_e\lambda_m^2 = 0, \tag{11}$$

where

$$A = \lambda_m(\eta_{zz} + s_z^2)(\varepsilon_{11}s_x^2 + \varepsilon_{22}s_y^2 + \varepsilon_{33}s_z^2) - 2\varepsilon_a\mu_a\eta_{zz}s_z^2, \quad \lambda_e = \varepsilon_{11}\varepsilon_{22} - \varepsilon_a^2, \tag{12a}$$

$$B = \varepsilon_{33}\lambda_m(\varepsilon_{11}s_x^2 + \varepsilon_{22}s_y^2) + \lambda_e\eta_{zz} + \varepsilon_{33}(\varepsilon_{11}\mu_{22} + \varepsilon_{22}\mu_{11} + 2\varepsilon_a\mu_a)s_z^2. \tag{12b}$$

It follows that in the medium, two distinct extraordinary waves can travel whose refractive indices are given by solutions of biquadratic equation (11). In general, for an arbitrary direction of propagation, both these waves are elliptically polarized and correspond to the coupled magnon–plasmon polaritons. In the following, we will restrict ourselves by consideration of the propagating waves in the case of the Voigt geometry.

3. Coupled magnon–plasmon polaritons in the case of the Voigt configuration

Consider the propagation of the waves in the xy-plane perpendicular to the magnetic field, so as s_z=0. In this case, the solutions of Eq. (11) are split in TM and TE waves with dispersion relations

$$n_{TM}^2 = \frac{\lambda_e}{\varepsilon_{11}s_x^2 + \varepsilon_{22}s_y^2} \tag{13}$$

and

$$n_{TE}^2 = \frac{\lambda_m \varepsilon_{33}}{\mu_{11}s_x^2 + \mu_{22}s_y^2}, \tag{14}$$

respectively. Let us consider first the TM wave in which the magnetic field vector **H** is parallel to the external field: **H**={0,0,H}. The electric field and time-averaged Poynting vector are given by

$$\mathbf{E} = (\omega\varepsilon_0\lambda_e)^{-1}\{-\varepsilon_{22}k_y - i\varepsilon_a k_x, \varepsilon_{11}k_x - i\varepsilon_a k_y, 0\}\mathrm{H}, \tag{15}$$

$$\mathbf{S} = \{\varepsilon_{11}k_x, \varepsilon_{22}k_y, 0\}(2\omega\varepsilon_0\lambda_e)^{-1}\left|\mathrm{H}\right|^2, \tag{16}$$

where

$$k_y^2 = (k_0^2\lambda_e - \varepsilon_{11}k_x^2)\varepsilon_{22}^{-1}, \quad k_0 = \omega/c. \tag{17}$$

Using Eqs. (16) and (17) we conclude that the dot product **kS**=$\omega\mu_0|\mathrm{H}|^2/2$ is positive. It means that propagating TM waves are always forward, but it does not mean that the phenomenon of negative refraction is impossible. Indeed, consider the case when $\varepsilon_{11} > 0$ while $\varepsilon_{22} < 0$, so as λ_ε is negative. It is not difficult to see that if TM wave is incident from the vacuum onto the interface of the medium, the transmitted bulk wave exists for all possible angles of incidence and the Poynting vector of the refracted wave is in the same side of the normal to the interface as that in the incident wave. Therefore, the negative refraction of the TM waves occurs without backward waves. Such a possibility of negative refraction has been predicted in [21] for uniaxial nongyromagnetic dielectrics with negative dielectric permittivity along the anisotropy axis.

It is important to note that TM waves correspond to the coupled plasmon polaritons without any mixture of the magnons. That is, why in the following we shall consider the peculiarities of the TE waves corresponding to the coupled magnon–plasmon polaritons, which are of interest in this work.

The field structure and time-averaged Poynting vector of the TE wave are given by

$$\mathbf{E} = \{0,0,\mathrm{E}\}, \quad \mathbf{H} = (\omega\mu_0\lambda_m)^{-1}\{\mu_{22}k_y + i\mu_a k_x, \ -\mu_{11}k_x + i\mu_a k_y, 0\}\mathrm{E}, \tag{18}$$

$$\mathbf{S} = \{\mu_{11}k_x, \mu_{22}k_y, 0\}(2\omega\mu_0\lambda_m)^{-1}|\mathrm{E}|^2, \tag{19}$$

where

$$k_y^2 = k_0^2\varepsilon_{33}\mu_v - \mu_{11}\mu_{22}^{-1}k_x^2 \tag{20}$$

and

$$\mu_v \equiv \frac{\lambda_m}{\mu_{22}} = \mu_{11} - \frac{\mu_a^2}{\mu_{22}} \tag{20a}$$

is the effective Voigt permeability. Using Eqs. (6b,6c), (2), (4a, 4b) and (9a), the dispersion relation (14) can be rewritten in the form

$$n^2 = \frac{\tilde{\varepsilon}(\omega^2 - \varpi_p^2)(\omega^2 - \Omega_+^2)(\omega^2 - \Omega_-^2)}{\omega^2(\omega^2 - \omega_+^2)(\omega^2 - \omega_-^2)}, \tag{21}$$

where

$$\tilde{\varepsilon} = \frac{l_1\varepsilon_\infty + l_2\varepsilon_A}{l_1 + l_2}, \tag{22}$$

$$\varpi_p = \omega_p\left(1 + \frac{l_2\varepsilon_A}{l_1\varepsilon_\infty}\right)^{-1/2}, \tag{23}$$

is the effective plasma frequency,

$$\omega_\pm^2 = \omega_0^2 + \omega_T^2 + \omega_A\omega_S \pm \sqrt{(\omega_A\omega_S)^2\left(1 - 4l_1l_2d^{-2}\sin^2\beta\right) + 4\omega_0^2(\omega_T^2 + \omega_A\omega_S)}, \tag{24}$$

β is the angle between the wave vector **k** and the positive y-axis: $\tan\beta = k_x/k_y$, and

$$\Omega_\pm^2 = \omega_0^2 + \omega_T^2 + \omega_A\omega_S(1 + l_2/d) \pm \sqrt{(\omega_A\omega_S)^2(l_1/d)^2 + 4\omega_0^2[\omega_T^2 + \omega_A\omega_S(1 + l_2/d)]}. \tag{25}$$

Using Eq. (21), it is easily seen that there are three branches in the spectrum of the TE waves, and in distinct ranges of the applied magnetic field these branches have different dispersion behaviors. In general, the magnetic fields can be divided into three distinct regions: "low" field ($\omega_0 < \omega_-^0$), "middle" ($\omega_-^0 \le \omega_0 \le \omega_+^0$) and "high" field ($\omega_0 > \omega_+^0$) regions. For a given direction of the wave propagation, the limits of these regions are defined by resonance frequencies at zero magnetic field

$$(\omega_\pm^0)^2 = \omega_T^2 + \omega_A\omega_S(1 \pm \sqrt{1 - 4l_1l_2d^{-2}\sin^2\beta}). \tag{26}$$

In the "low" and "high" field regions, the wave has two resonance frequencies ($n \to \infty$) at $\omega = \omega_+$ and $\omega = \omega_-$ while in the "middle" field regime there is only one resonance at $\omega = \omega_+$.

With increase in magnetic field, ω_+ increases monotonically while ω_- decreases in the range of the "low" fields, vanishes at $\omega_0 = \omega_-^0$, appears again at $\omega_0 = \omega_+^0$ and then increases approaching asymptotically the straight line $\omega = \omega_0$ in the range of the "high" fields (see Fig. 2, solid lines). Besides, the wave has three cutoff frequencies (n=0) at $\omega = \varpi_p$ and $\omega = \Omega_\pm$. The dependence of $\Omega_\pm$ on the magnetic field is shown schematically in Fig. 2 (dashed curves).

Note that the "middle" field region is very narrow: for MnF_2, inserting in Eq. (26) l_1=1 μm, l_2=0.2 μm, $\beta = \pi/6$, ω_S=1.722 GHz

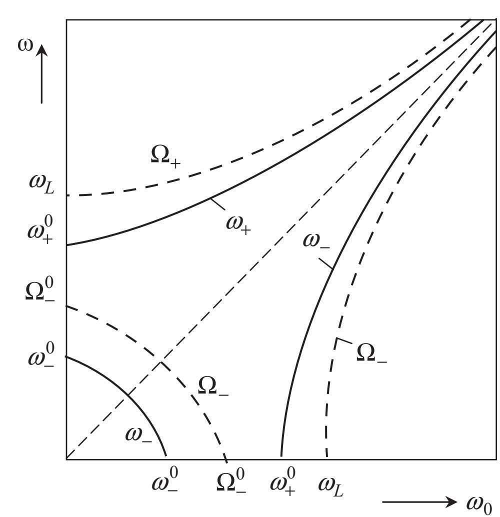

Fig. 2. Schematic plot of the resonance (solid lines) and cutoff (dashed lines) frequencies versus ω_0.

and using the parameter values given in Eq. (4d), we obtain

$$\omega_-^0 = 185.877\,\text{GHz}, \quad \omega_+^0 = 185.971\,\text{GHz}, \tag{26a}$$

that is, 64.76 kG $< H_0 <$ 64.80 kG. In spite of that, the "middle" field region should be divided in two parts

$$\text{(I)} \quad \omega_-^0 \le \omega_0 < \Omega_-^0 \tag{27a}$$

and

$$\text{(II)} \quad \Omega_-^0 \le \omega_0 \le \omega_+^0, \tag{27b}$$

where

$$\Omega_-^0 = \sqrt{\omega_T^2 + 2\omega_A\omega_S l_2/d} \tag{28}$$

is the cutoff frequency at zero magnetic field. An estimation for MnF_2 gives $\Omega_-^0 = 185.891$ GHz. In part I, the wave has three cutoff frequencies while in part II there are only two such frequencies.

In Fig. 3, the dispersion curves in the "low" field regime are shown schematically for three different values of the plasma frequency: $\varpi_p < \omega_-$ (Fig.3a), $\omega_- < \varpi_p < \Omega_-$ (Fig.3b) and $\omega_+ < \varpi_p < \Omega_+$ (Fig.3c). The wave exists, as in the absence of the magnetic field, in three frequency regions, the limits of which are different for these three cases and also depend essentially on the magnetic field. Note that the dispersion of the high-frequency branch is normal in all these three cases while that for the low-frequency branch is anomalous ($\partial\omega/\partial k < 0$) in cases (b) and (c). As to the middle branch, it is normal in cases (a), (b) and anomalous in case (c). It is evident that left-handed behavior of the medium can only be expected in the frequency ranges corresponding to the branches with anomalous dispersion.

In Figs. 4 and 5, the dispersion curves of the TE wave are shown in the "middle" field regime for different values of the plasma frequency in part I [see Eq. (27a), Fig. 4] and part II [Eq. (27b), Fig. 5). In the latter case, there are only two branches in the spectrum, and low-frequency branch possess anomalous dispersion only if the condition

$$\varpi_p > \omega_+ \tag{29}$$

is fulfilled (see Figs. 5b, c). Note that in part I of the "middle" field range, there is only one branch with anomalous dispersion for $\omega_p < \Omega_-$ (Fig. 4a) and two such branches for$\omega_p > \omega_+$ (Fig. 4b). Note also that unlike the cases shown in Figs. 3 and 5, the wave numbers for the low-frequency branch in Fig. 4a, b are restricted: $k < k^\sim$, where

$$\tilde{k} = \varpi_p(\varepsilon_0\mu_0\tilde{\varepsilon}\rho)^{1/2}, \quad \rho = \frac{(\omega_L^2-\omega_0^2)(\omega_T^2+2\omega_A\omega_S l_2 d^{-1}-\omega_0^2)}{(\omega_L^2-\omega_0^2)(\omega_0^2-\omega_T^2)-4\omega_A^2\omega_S^2 l_1 l_2 d^{-2}\sin^2\beta}. \tag{30}$$

However, the last statement is only true if $\omega_0 > \omega_-^0$. At $\omega_0 = \omega_-^0$, the low-frequency branch exists for all possible wave numbers and approaches asymptotically to zero when $k \to \infty$.

Finally, "high" field region should be divided in two subregions too: $\omega_+^0 < \omega_0 \le \omega_L$ and $\omega_0 > \omega_L$, where

$$\omega_L = (\omega_T^2 + 2\omega_A\omega_S)^{1/2} \tag{31}$$

is the frequency of the longitudinal optical magnons at zero magnetic field. Substituting in Eq. (31)ω_T=185.874 GHz, ω_A=10.906 GHz and ω_S=1.722 GHz (MnF_2), we obtain ω_L=185.975 GHz. The wave has two cutoff frequencies in the first part and three in the second one. In Fig. 6, the dispersion curves are shown in both these subregions for the case when $\omega_+ < \varpi_p < \Omega_+$. Note that in the frequency range $\omega_+ < \omega < \varpi_p$ there is only one branch with anomalous dispersion, and low-frequency branch in the case of Fig. 6a exists only if the wave number $k > k^\sim$, where $k^\sim$ is given by Eq. (30).

The estimated values of the resonance, cutoff and cyclotron frequencies are shown in Table 1.

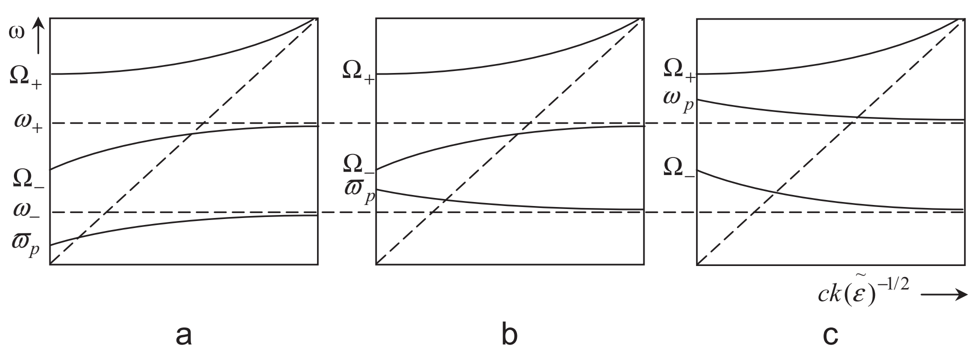

Fig. 3. Dispersion curves in "low" field regime for different values of the effective plasma frequency. (a) $\varpi_p < \omega_-$; (b) $\omega_- < \varpi_p < \Omega_-$; (c) $\omega_+ < \varpi_p < \Omega_+$.

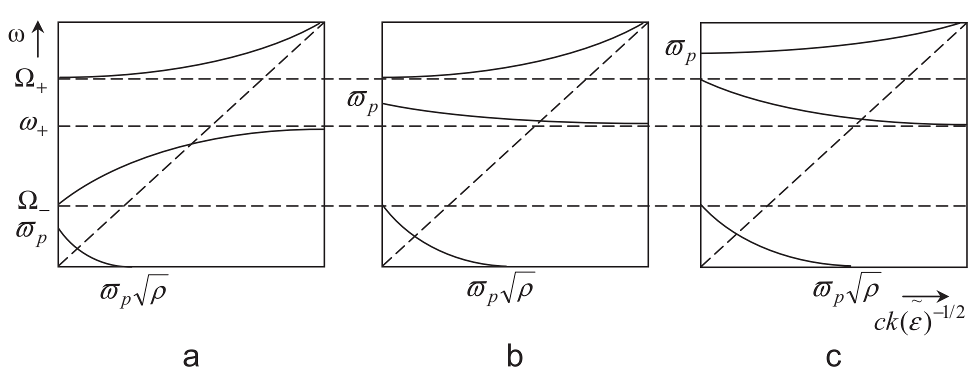

Fig. 4. Dispersion curves in part I of the "middle" field regime. (a) $\varpi_p < \Omega_-$; (b) $\omega_+ < \varpi_p < \Omega_+$; (c) $\varpi_p > \Omega_+$.

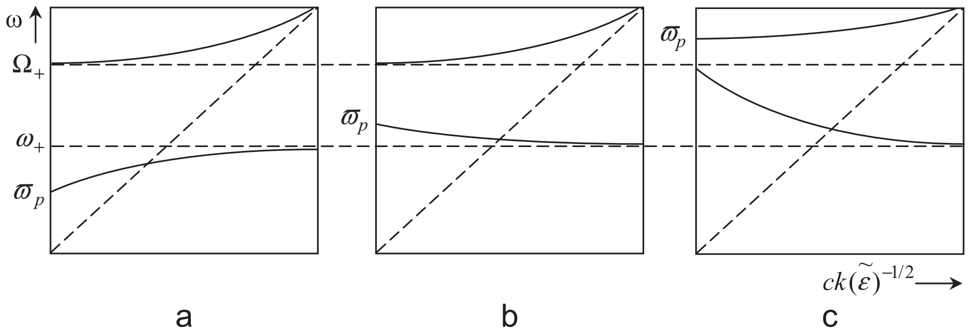

Fig. 5. Dispersion curves in part II of the "middle" field regime. (a) $\varpi_p < \omega_+$; (b) $\omega_+ < \varpi_p < \Omega_+$; (c) $\varpi_p > \Omega_+$.

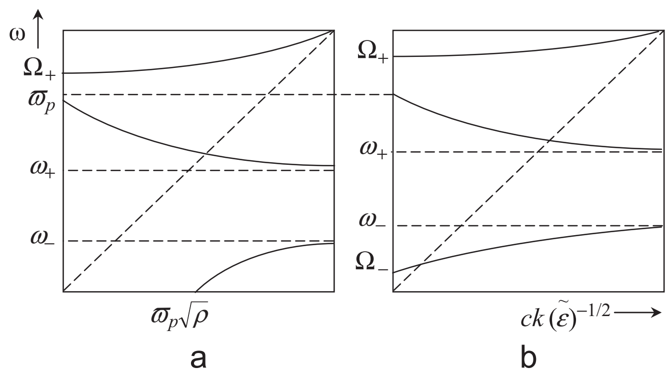

Fig. 6. Dispersion curves in different parts of "high" field regime. (a) $\omega_+^0 < \omega_0 \le \omega_L$. (b) $\omega_0 > \omega_L$.

Table 1
The estimated values of the resonance($\omega_\pm$), cutoff ($\Omega_\pm$) and cyclotron (ω_c) frequencies for SL MnF_2 /CdTe at six different values of the field H_0 (two values for each field region). The effective mass of the conducting electrons in CdTe m=0.11 m_0; ε_∞=10.

H_0(kG s)	ω_0(GHz)	ω_-(GHz)	ω_+(GHz)	Ω_-(GHz)	Ω_+(GHz)	ω_c(GHz)
0.3	0.861	185.063	186.786	185.072	186.794	7.63
30	86.1	99.822	272.025	99.833	272.033	763.47
64.767	185.88	–	371.804	0.355	371.813	1648
64.780	185.92	–	371.844	–	371.852	1648.59
64.799	185.973	0.764	371.911	–	371.919	1649
65.157	187	1.039	372.925	0.969	372.933	1658.19

We see that all the values of the characteristic parameters are much far from the cyclotron frequency. Note also that the interesting frequency regions with anomalous dispersion in Figs. 4c and 5c may be difficult to realize experimentally if the effective plasma frequency ϖ_p is below Ω_+. Using the estimates for Ω_+ in Table 1 and substituting l_2/l_1=0.2, ε_∞=10(CdTe) and ε_A=5.5(MnF_2) in the formula for ϖ_p [see Eq. (23)], we obtain that the situations shown in Figs. 4c and 5c ($\varpi_p > \Omega_+$) can only be accessible if the density of the free charge carriers in semiconductor layers $N > 5.3 \times 10^{19}\ \mathrm{m}^{-3}$. Moreover, the frequency regions shown in Fig. 6, where $\omega_+ < \varpi_p < \Omega_+$, can only be realized experimentally if $5.332 \times 10^{19} < N < 5.333 \times 10^{19}(\mathrm{m}^{-3})$. However, in most of other cases shown in Figs. 3–6, the value of the plasma frequency can be high enough and the corresponding frequency regions are perfectly accessible. Taking into account that the density of the free charge carriers depends strongly on the temperature, as well as on the type of impurities and the doping level and therefore can be varied in the wide interval, we can be sure that the necessary values of the effective plasma frequency are fully reachable.

4. Necessary conditions for the negative refraction of the TE waves. Phase and group refractive indices

Suppose now that TE type polarized plane wave $\mathbf{E},\mathbf{H} \sim \exp[i(k_{0x}x + k_{0y}y - \omega t)]$ is incident from the vacuum onto the interface of the medium. For a given value α of the angle of incidence, $k_{0x}=k_0 \sin\alpha$ and $k_{0y}=k_0\cos\alpha$. Inside the medium, the refracted wave propagates as mixed magnon–plasmon polariton of the same polarization.

Using Eqs. (19) and (20), for the dot product of the wave and Poynting vectors we obtain

$$\mathbf{kS} = \frac{(\mu_{11}k_x^2 + \mu_{22}k_y^2)}{2\omega\mu_0\mu_{22}\mu_v}|E|^2 = \frac{1}{2}\omega\varepsilon_0\varepsilon_{33}|E|^2. \tag{32}$$

Taking into account that the energy flux for the refracted wave is always directed away from the interface ($s_y > 0$), we conclude that the wave is backward with respect to the interface (i.e., the phase velocity is directed to the interface) only if the condition

$$\mu_v < 0 \tag{33a}$$

is fulfilled. At this end, the medium is left-handed with respect to the wave (i.e., $\mathbf{kS} < 0$), if

$$\varepsilon_{33} < 0, \tag{33b}$$

and the negative refraction occurs if

$$\mu_{11}\mu_{22} > 0. \tag{33c}$$

Except that, the condition of existence for the refracted wave ($k_y^2 > 0$) must be fulfilled

$$\varepsilon_{33}\mu_v > \frac{\mu_{11}}{\mu_{22}}\sin^2\alpha. \tag{33d}$$

All these four conditions (33a–d) can only be fulfilled simultaneously within the frequency bands of anomalous dispersion. The corresponding situation in Ref. [13] has been termed as the case of absolute left-handed medium. The mutual orientation of the wave and Poynting vectors in this case is illustrated schematically in Fig. 7. The angles of refraction for the wave and Poynting vectors are given by Snell's law $\sin\beta = n_p^{-1}\sin\alpha$ and $\sin\gamma = n_g^{-1}\sin\alpha$, respectively, where

$$n_p = \sqrt{\varepsilon_{33}\mu_v + (1 - \mu_{11}/\mu_{22})\sin^2\alpha} \tag{34}$$

is the phase refractive index and

$$n_g = -\sqrt{\varepsilon_{33}\mu_v(\mu_{22}/\mu_{11})^2 + (1 - \mu_{22}/\mu_{11})\sin^2\alpha} \tag{35}$$

is the group refractive index. The angle ϕ between the wave and Poynting vectors is given by

$$\cos\varphi = \frac{\sin^2\alpha + \sqrt{(n_p^2 - \sin^2\alpha)(n_g^2 - \sin^2\alpha)}}{n_p n_g} \tag{36}$$

and is always obtuse if the conditions (33a–d) are fulfilled.

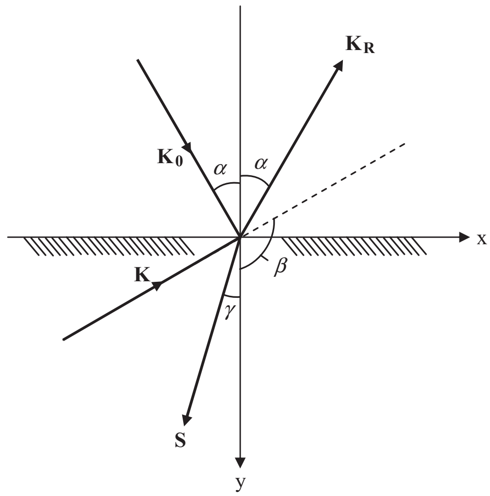

Fig. 7. Mutual orientation of the wave and Poynting vectors in the negatively refracted TE wave. $\mathbf{K}_0$ and $\mathbf{K}_R$ are the wave vectors for the incident and reflected waves, respectively.

It is remarkable that the TE-wave can be refracted negatively even when it is forward (with respect to the interface) and the wave and Poynting vectors make an acute angle ($\mathbf{kS}>0$). Such a situation is only possible if the following conditions are fulfilled simultaneously:

$$\mu_v>0, \quad \varepsilon_{33}>0, \quad \mu_{11}>0, \quad \mu_{22}<0, \tag{37}$$

Indeed, using Eq. (19), it is easily to see that in this case the Poynting vector of the refracted wave is in the same side of the normal to the interface as that in the incident wave, that is, the negative refraction of the TE waves occurs without backward waves.

5. Conclusions

Using the method of effective anisotropic homogeneous medium, the effective permittivity and permeability tensors are obtained for the periodic multilayer structures consisting of alternating layers of nonmagnetic semiconductor and nonconducting antiferromagnet, in the presence of an external magnetic field parallel to the surface of the layers. It is shown that there are a few frequency bands where the structure under consideration behaves as a negative-index left-handed medium. In the case of the Voigt configuration, when TE- and TM-type refracted waves are propagated separately, the TM waves correspond to the coupled plasmon polaritons without any mixture of the magnons; the waves are always forward and can only be negatively refracted if the permittivity along the normal to the interface is negative. The TE waves correspond to the mixed magnon–plasmon polaritons whose dispersion properties are very sensitive to the applied magnetic field. The relative orientation of the Poynting and wave vectors in the TE wave is examined in different frequency ranges and different regimes of the applied field. In general, the behavior of the wave depends on the sign of the Voigt permeability, diagonal components of the effective permeability tensor in the plane perpendicular to the applied field and effective permittivity ε_{33} along the field direction. It is shown that the wave is backward and can be refracted negatively if the following conditions are fulfilled simultaneously: (a) ε_{33} should be negative; (b) instead of the scalar permeability in isotropic case, the effective Voigt permeability must be negative; (c) the additional conditions (33c,d) should be fulfilled too. We have shown also that the structure with negative permeability along the normal to the interface can achieve negative refraction with respect to the TE wave even when the wave is forward.

The main properties of the wave, in particular, the number of the frequency bands of propagation, their limits and width, as well as the number of the branches with anomalous dispersion are quite different in various ranges of the applied magnetic field and therefore can be changed using the latter as a tuning parameter. It is remarkable that the limits of the frequency regions of the anomalous refraction are very sensitive not only to the applied field but also to the effective plasma frequency. This fact opens possibility for control of the regions using the samples with different values of the free charge carrier's density in the semiconductor layers.

Acknowledgement

The authors would like to thank Professor C. Soukoulis for his encouragement and useful discussions.

References

[1] V.G. Veselago, Sov. Phys. Usp. 10 (1968) 509–514.
[2] J.B. Pendry, Phys. Rev. Lett. 85 (2000) 3966–3969.
[3] R.A. Shelby, D.R. Smith, S. Schultz, Science 292 (2001) 77.
[4] P. Markos, C.M. Soukoulis., Phys. Rev. B 65 (2001) 033401;
P. Markos, C.M. Soukoulis., Opt. Express 11 (2003) 649–661.
[5] S. Tretyakov, I. Nefedov, A. Sihvola, S. Maslovski, C. Simovski, J. Electromagn. Waves Appl. 17 (2003) 695.
[6] S. Foteinopoulou, C.M. Soukoulis, Phys. Rev. B 72 (2005) 165,112.
[7] S. Tretyakov, A. Sihvola, L. Jylha, Photonics Nanostruct. Fundam. Appl. 3 (2005) 107.
[8] C.M. Soukoulis, S. Linden, M. Vegener, Science **315** (2007) 47.
[9] V.M. Agranovich, Yu.N. Gartstein, A.A. Zakhidov, Phys. Rev. B 73 (2006) 045,114.
[10] I.V. Shadrivov, A.A. Zharov, Yu.S. Kivshar, Opt. Soc. Am. B 23 (2006) 529.
[11] V.M. Shalaev, Nat. Photon 1 (2007) 41.
[12] R.H. Tarkhanyan, D.G. Niarchos, Opt. Express 14 (2006) 5433;
R.H. Tarkhanyan, D.G. Niarchos, Phys. Status Solidi (b) 245 (2008) 154–158.
[13] R.H. Tarkhanyan, D.G. Niarchos, J. Magn. Magn. Mater. 312 (2007) 6–15.
[14] R.H. Tarkhanyan, D.G. NiarchosPhys. Status Solidi (b) 246 (2009) 1939–1944.
[15] D.L. Mills, E. Burstein, Rep. Prog. Phys. 37 (1974) 817.
[16] V.M. Agranovich, D.L. Mills (Eds.), 1982.
[17] F. Keffer, C. Kittel, Phys. Rev. 85 (1952) 329.
[18] R.E. Camley, D.L. Mills, Phys. Rev. B26 (1982) 1280.
[19] V.M. Agranovich, V.E. Kravtsov, Solid State Commun. 55 (1985) 85.
[20] D.J. Bergman, X. Li, Y.M. Strelniker, Phys. Rev. B 71 (2005) 035,120.
[21] P.A. BelovMicrowave Opt. Technol. Lett. 37 (2003) 259–262.